Mechanochemically-Driven Self-Assembly of a Chiral Mono-Biotinylated Hemicucurbit[8]uril

Elina Suut-Tuule,[a]‡ Tatsiana Jarg,[a]‡ Priit Tikker,[b] Ketren-Marlein Lootus,[a] Jevgenija Martõnova,[a] Rauno Reitalu,[a] Lukas Ustrnul,[a] Jas S. Ward,[c] Vitalijs Rjabovs,[d,e] Kirill Shubin,[f] Jagadeesh V. Nallaparaju,[a] Marko Vendelin,[g] Sergei Preis,[b] Mario Öeren,[a] Kari Rissanen,[c] Dzmitry Kananovich,[a] and Riina Aav[a]*

[a]*Tallinn University of Technology, Department of Chemistry and Biotechnology, Akadeemia tee 15, 12618 Tallinn, Estonia*

[b]*Tallinn University of Technology, Department of Materials and Environmental Technology, Ehitajate tee 5, 19086 Tallinn, Estonia*

[c]*University of Jyvaskyla, Department of Chemistry, 40014 Jyväskylä, Finland*

[d]*National Institute of Chemical Physics and Biophysics, Akadeemia tee 23, 12618 Tallinn, Estonia*

[e]*Institute of Technology of Organic Chemistry, Riga Technical University, P. Valdena str. 3, LV-1048, Riga, Latvia*

[f]*Latvian Institute of Organic Synthesis, Aizkraukles str. 21, LV-1006, Riga, Latvia*

[g]*Tallinn University of Technology, Department of Cybernetics, Laboratory of Systems Biology, Akadeemia tee 15, 12618 Tallinn, Estonia*

*Corresponding author: Riina Aav, riina.aav@taltech.ee.

Abstract: Hemicucurbiturils are macrocycles formed by connecting ethyleneurea moieties with methylene bridges. This study presents the development of self-assembled chiral mono-biotinylated hemicucurbit[8]urils (mixHC[8]) in the solid state. The mixHC[8]s were synthesized in a single preparative step by a mechanochemically-assisted condensation reaction of D-biotin, (*R*,*R*)- or (*S*,*S*)-cyclohexa-1,2-diylurea and formaldehyde. Dynamic covalent library of over 100 identified oligomers was generated via ball milling under perchloric or hexafluorophosphoric acid catalysis. Rigorous analysis of intermediates, including formation kinetics of short oligomers, revealed key processes and chemical parameters influencing self-assembly. We found that self-organization of about 50,000 theoretically predicted oligomers can be directed to formation of 8-membered hemicucurbiturils in 75% yield, consisting of a 1:1 mixture of chimeric mixHC[8] and homomeric cyclohexanohemicucurbit[8]uril (cycHC[8], 38% and 37% yields, respectively), or predominantly homomeric cycHC[8] (up to a 72% yield). The developed procedure was used for synthesis of diastereomeric (−)- and (+)-mixHC[8] suitable for anion binding and derivatization. Immobilization of mixHC[8] on a surface of aminated silica produced a functional material capable of selective capture of anions, as demonstrated by efficient perchlorate removal from a spiked mineral matrix.

Keywords: Mechanochemistry; Self-Assembly in Solid State; Dynamic Covalent Chemistry; Hemicucurbituril; Perchlorate Binding.

Introduction

The spontaneous organization of molecular species relies on non-covalent interactions, resulting in intricate aggregates. Such supramolecular self-assembly can facilitate the formation of covalent bonds leading to complex molecules, and may be exceptionally responsive to minor changes in the external stimuli, resulting in the amplification of particular products.[1] Under conditions of increased molecular crowding, the dynamics of interaction between species is accelerated compared to a dilute environment, which has been demonstrated for strongly hydrogen-bonded base pairs of nucleic acids.[2] Furthermore, at extreme concentrations in the solid state, where non-covalent interactions are stronger, the formation of products that are less favorable in solution can occur.[3,4] Mechanochemical activation enhances chemical reactivity and provides a solvent-free sustainable approach in chemical syntheses.[5–7]

Single-bridged cucurbituril-type molecular containers, hemicucurbit[*n*]urils (HC[*n*]s) are renowned for their anion-binding properties and are typically assembled from urea monomers in a one-pot reaction with dynamic covalent chemistry (DCC).[8–10] Although the size of the macrocycle can be controlled by anion templation,[8,11–15] HCs prevalently consist of six units.[12,16,17] Up to date, 8-membered HCs have been synthesized exclusively from chiral C_2-symmetric cyclohexa-1,2-diylurea (CU) monomers, and the corresponding (*R*,*R*)- and (*S*,*S*)-cyclohexanohemicucurbit[8]urils (cycHC[8]) can be assembled both in solution[18] and the solid state[17]. Their larger cavity expands the range of applications, and insertion of another functional monomer, such as D-biotin, into cycHC[8] scaffold can further enhance receptor versatility. Biotin is a naturally occurring and commercially available compound with a carboxylic group suitable for derivatization. Furthermore it has previously been used in the synthesis of chiral macrocycles[13]. So far, the reported chimeric HCs assembled from non-equivalent urea monomers have been limited to six-membered hybrid HCs prepared in solution via multi-step approaches,[19,20] and mono-functionalized bambus[6]urils obtained in a one-pot reaction.[21–23] The difficulties in the single-step formation of non-uniform oligomeric macrocycles arise from a plethora of possible linear

and cyclic intermediates. Consequently, arranging a chaotic mixture into a well-organized molecule presents considerable challenges, and the number of combinations increases with the number of monomeric units.

Mechanochemistry has been utilized in the synthesis of several macrocycles,[17,24–30] inducing covalent self-assembly of uniformly structured monomers. As mechanosynthesis enables overcoming the solubility barriers and promotes reactions between compounds with drastic polarity differences, its potential can be exploited even further. To the best of our knowledge, there have been no reports describing solid-state formation of oligomeric macrocycles from mixtures of various monomers. Formation of chiral chimeric HCs via self-assembly in the solid state could pave the way to novel synthetic approaches, unlocking access to versatile applications.

The present work describes a mechanochemically-activated solid-state condensation of (*R,R*)- or (*S,S*)-cyclohexa-1,2-diylurea (CU), D-biotin ((*S,S,R*)-B) and paraformaldehyde, and their selective self-assembly into enantiopure mono-biotinylated hemicucurbit[8]urils (−)-((*S,S,R*)(*R,R*)$_7$)-mixHC[8] or (+)-((*S,S,R*)(*S,S*)$_7$)-mixHC[8] along with homomeric cycHC[8]. The challenges of assembling a chimeric mono-functionalized 8-membered macrocycle are related to the number of possible combinations of monomeric units and their chemical reactivity. Fine-tuning of the reaction conditions enabled amplification of the two major products - chimeric mixHC[8] and homomeric cycHC[8], among 498 potential 8-membered HCs[31] (Figure 1).

The covalent self-assembly process was essentially solvent-free and with a very low process mass intensity (PMI, the mass of all used reagents per formed product[32]). The most significant chemical and technical factors affecting macrocyclization were identified with response surface methodology (RSM), and thorough analysis of intermediates by HPLC-MS provided mechanistic insight to this complex process. The affinity of mixHC[8] for selected anions and the subtle differences in the binding properties of the two new chimeric diastereomers were determined by isothermal titration calorimetry (ITC) and their structures characterised by single-crystal X-ray crystallography (SC-XRD) and modelling

studies. Furthermore, a practical example of the selective anion capture by silica-immobilized mixHC[8] was demonstrated in the efficient removal of perchlorate from a spiked mineral matrix.

Results and Discussion

Self-assembly of hemicucurbiturils in the solid state

The first attempts to synthesize mono-functionalized mixHC[8] in solution according to the protocol developed for cycHC[8][18] were promising. The condensation of biotin and CU taken in stoichiomeric 1:7 molar ratio with paraformaldehyde, mediated by trifluoroacetic acid in acetonitrile, produced mixHC[8] and cycHC[8] in 10% and 38% yields, respectively (see SI S4). The ratio of the macrocycles did not reflect the statistical distribution based on the starting monomer ratio, which implied a strong influence of the chemical parameters. We envisioned that mixHC[8] may be assembled with higher efficiency in the solid state, where templation is enhanced due to a high concentration of reactants and the desolvation effect.[3] According to the previous study,[17] self-assembly in the solid state required just a minute amount of a liquid additive[33–35] to facilitate proton transfer and delivery of the anionic template, as well as to promote conformational flexibility. The complexity of a dynamic covalent library (DCL) drastically increases in multi-component reactions, for instance, incorporation of non-C_2 symmetric (*R,S*)-cyclohexa-1,2-diylurea units resulted in higher stereochemical diversity and the formation of several diastereomeric HCs (*i.e*, *cis*-cycHC[6] and *inverted-cis*-cycHC[6]).[36] Similarly, self-assembly of chiral CU and non-C_2 symmetric biotin into linear and cyclic oligomers can be realized via various combinations, considering the possibilty of different orientations of the biotin unit (see SI S3). For instance, all forms with the length from 2 to 10 result in *ca.* 50,000 cyclic and linear oligomers. However, the number of possible products can be decreased by templation. Variation of position, orientation and number of B and CU monomers leads to 498 potential 8-membered macrocycles[31] (Figure 1, see SI S5). Full conversion of the 1:7 ratio of B and CU into HC[8]s is expected to direct 498

combinations to 12% and 82% of mixHC[8] and cycHC[8], respectively (Figure 1, and SI Table S1).

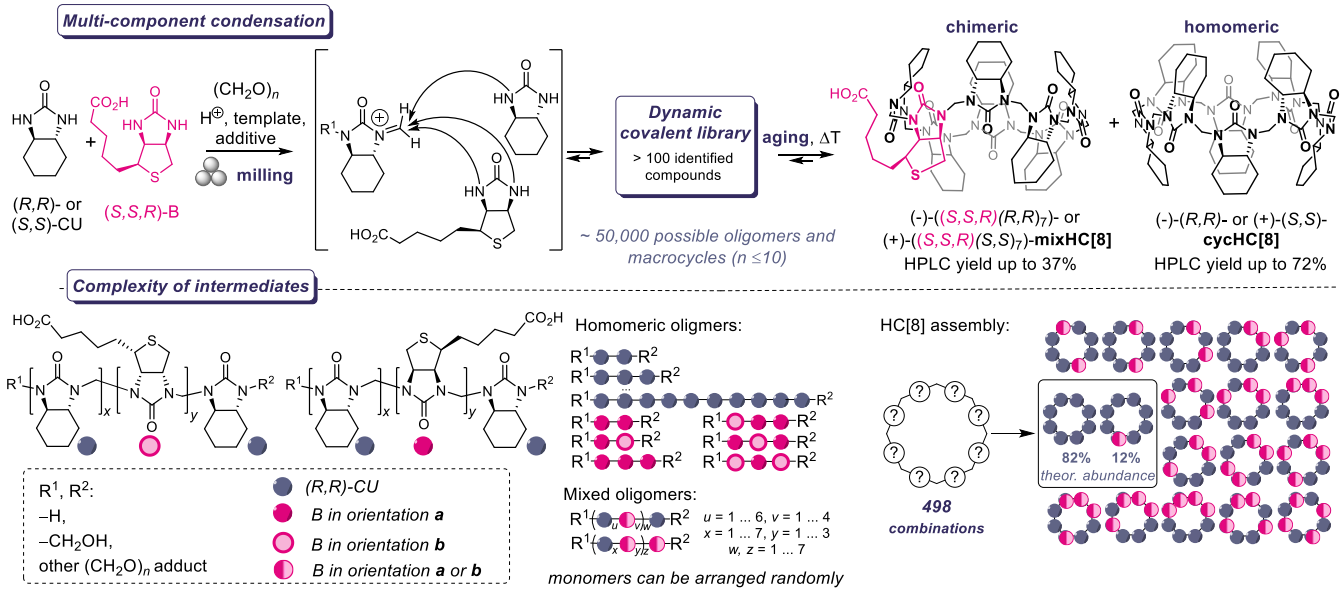

Figure 1. Multi-component condensation of (*S,S,R*)-biotin (B) and (*R,R*)- or (*S,S*)-cyclohexa-1,2-diylurea (CU) to homomeric cycHC[8] and chimeric mixHC[8]s shown in this work. Complexity of intermediates in the dynamic covalent library is expressed via possible number of combinations of oligomers, HC[8]s and the abundance of major HC[8]s from the 1:7 (B:CU) ratio of starting materials. Best reaction conditions, affording 37% and 38% yields of mixHC[8] and cycHC[8], respectively: 1 eq. B, 7 eq. CU, 8 eq. $(CH_2O)_n$ in presence of 2 eq. HPF_6. and 1 eq. KPF_6, milled at 30 Hz for 60 min and aged at 60°C for 24h.

The fact that solution phase synthesis did not result in a statistical ratio of more favored HC[8]s, encouraged us to study if the selectivity of mono-biotinylated mixHC[8] formation can be increased via tuning the parameters of the mechanochemical reaction. To investigate the effect of multiple external stimuli on the assembly of 8-membered macrocycles, we utilized RSM for experimental design and the screening of reaction conditions.[37] The HPLC yields of mixHC[8] and cycHC[8] obtained after the aging step were plotted as 3D response surfaces, highlighting the conditions favorable for the assembly of mixHC[8] compared to cycHC[8] (Figure 2A-B, Tables S2–S6, Figures S3–S7). The ratio of monomers, loading of aqueous mineral acid ($HClO_4$), milling duration, and aging temperature, which affect CU macrocyclization,[8] were simultaneously explored.

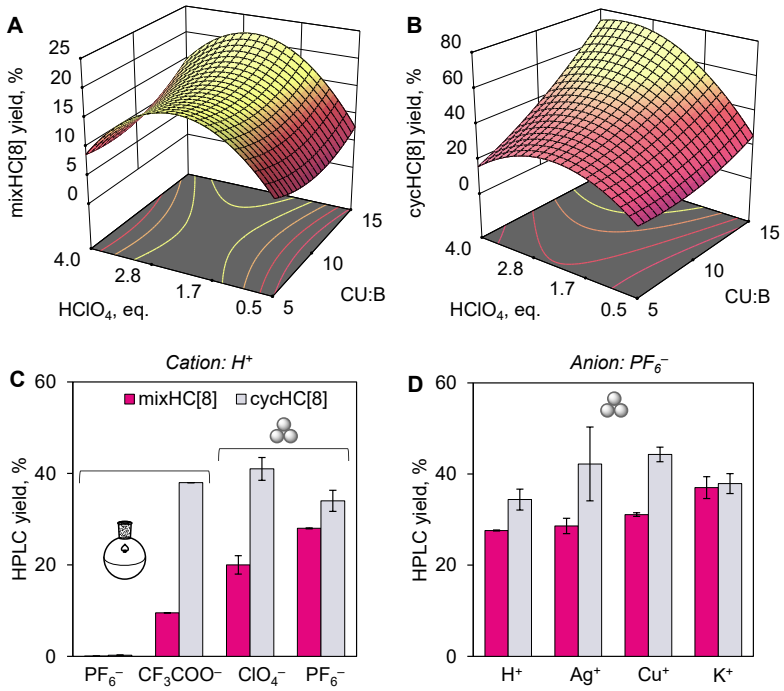

Figure 2. 3D response surfaces displaying the influence of the ratio of monomers and loading of aq. $HClO_4$ on the HPLC yields of (A) mixHC[8] and (B) cycHC[8]. Bar charts comparing the effect of the acid anions (CF_3COO^-, ClO_4^- and PF_6^-) in solution and the solid state (C) and hexafluorophosphate salt cations (Ag^+, Cu^+, K^+) in the solid state (D) on the yields of cycHC[8] (gray) and mixHC[8] (magenta). For more details, see Table S7 in the SI.

The formation of mixHC[8] and cycHC[8] proved to be sensitive to the monomer ratio and acid loading (Figure 2A-B). Variations of the monomer ratios within the range from 1:5 to 1:15 did not significantly affect the yield of chimeric mixHC[8] (Figure 2A, Table S13), however, using an excess of CU clearly resulted in the enhanced generation of cycHC[8] (Figure 2B, Table S13). The quantity of $HClO_4$ appeared as the vital parameter affecting the formation of mixHC[8]. The highest yields of mixHC[8] were attained within the specific range of $HClO_4$ loadings of 1.2–3.0 eq. (Figure 2A), while cycHC[8] was less dependent on the quantity of acid catalyst. This observation highlights the difference in formation of mixHC[8] and cycHC[8] in response to varied reaction conditions. The impacts of milling time and aging temperature appeared to be less significant, and the optimal temperature for ripening mixHC[8] was found to range from 40 to 65°C. RSM helped to reach a 20% yield of mixHC[8] under standard conditions – 3 eq. of template, 1 h ball-milling followed by 24 h aging at 60 °C – selected for further optimization studies.

It was hypothesized that an alternative template could amplify the formation of the target macrocycle. The binding studies for the cycHC[8] receptor revealed the following ranking of anion affinity: $SbF_6^- > PF_6^- > ReO_4^- > ClO_4^-$.[11] The use of hexafluoroantimonate (SbF_6^-) as a template did not seem practical, since $HSbF_6$ mainly exists as the HF/SbF_5 superacid system.[38,39] Hexafluorophosphate (PF_6^-), on the other hand, serves as an efficient template for the synthesis of homomeric cycHC[8] in solution.[18] Due to its advantageous templating potential, HPF_6 was chosen as an alternative reagent to mediate the solid-state synthesis of mixHC[8]. In addition, it is safer to handle compared to perchlorates that are known for their undesirable oxidative, flammable and explosive hazards.[40,41] Interestingly, the use of HPF_6 resulted in decreased formation of homomeric cycHC[8], contrary to an improved yield (28%) of mixHC[8] (Figure 2C, Table S7). Since the self-assembly of mixHC[8] was highly sensitive to the quantity of acid (Figure 2A), we tested three hexafluorophosphate salts ($AgPF_6$, $[Cu(CH_3CN)_4]PF_6$, KPF_6) as additives to partially substitute the acid while keeping the amount of template anion constant (Figure 2D, Table S7). Additionally, we anticipated that the Ag^+ and Cu^+ cations could serve as potential promoters for the generation of mixHC[8] due to their affinity for biotin.[42–44] As depicted in Figure 2D, the Ag^+ and Cu^+ salts had a negligible effect on formation of mixHC[8], while improving the yield of homomeric cycHC[8] compared to the reaction with HPF_6. The latter points at the effective decrease in the concentration of antagonistic[45] CU-rich mixed oligomers, which reassembled and provided CU to cyclize into cycHC[8]. The best result was achieved with KPF_6, which afforded the highest yield of mixHC[8] (37%), with accompanying formation of cycHC[8] (38%) (Figure 2D). Further variation of HPF_6/KPF_6 equivalence by RSM, however, did not improve the formation of mixHC[8] (see SI, Tables S8–S12, Figure S8). Once the key chemical parameters had been identified, the duration of ball-milling and aging at moderately elevated temperatures were optimized (see Tables S14–S15).

The changes in the content of intermediates and products were analyzed by HRMS. Altogether, over 100 reaction species were identified in the crude reaction mixtures during different stages of covalent self-assembly and mapped based on MS signal intensities (Figure 3a, Table S16, Figures S9–S13, MatchMass tool[46]). The results display the

dynamic changes in the composition of the reaction mixture during milling and aging. Biotin was found to be incorporated into different linear oligomers $(CU)_x(B)_y$ ($x = 1…7$, $y = 1…4$), as well as into a number of mono-, di-, tri- and tetra-biotinylated mixHC[n] ($n = 6…8$). Homomeric CU oligomers dominate at the initial phase of the polycondensation reaction (milling time: 5 min) and are kinetically favored products. Consequently, the milling time must be sufficient (60 min, see Tables S14-S15) to enable the accumulation of the slowly generated mixed biotin-containing oligomers. The content of the mixed oligomers ($n = 6–8$), which are essential for mixHC[n] formation, significantly increased after 45–60 minutes milling. This difference in the contents of the short- and long-milled mixtures emphasizes the dynamic shuffling of the monomers, which resulted in an increased random distribution of biotin upon prolonged milling. The low content of macrocycles in DCL directly after milling can be attributed to the unfavorable complexation with the template,[11,17] most likely due to increased entropy during mechanical agitation. The macrocyclic products predominantly ripened at the aging stage, at which point the mixed and homomeric oligomers underwent additional, although less intense crossover unit exchange.

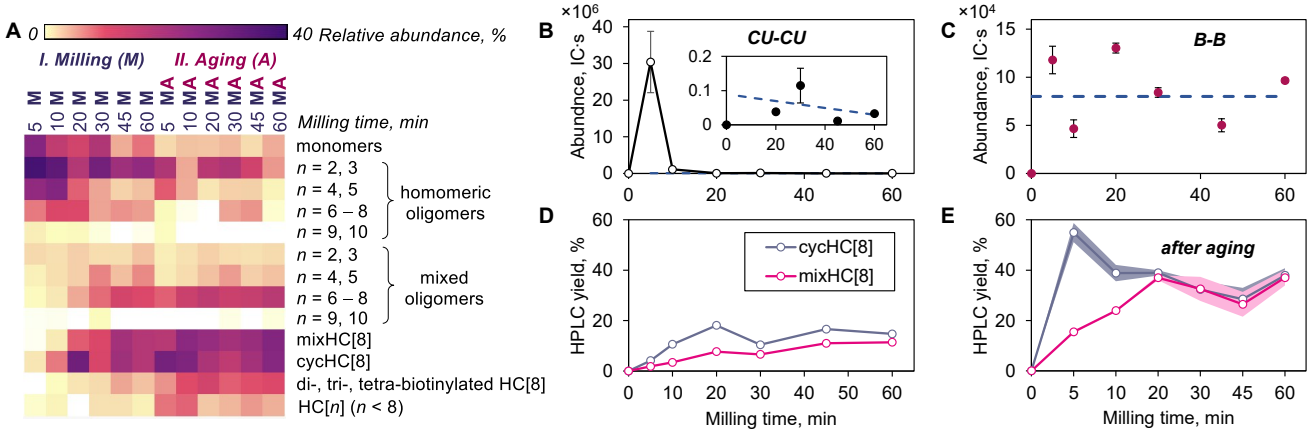

Figure 3. DCL composition summarized in a heatmap (A) based on MS abundance of detected species (S17–S30, Table S16 and Figure S13); content of homomeric dimers CU-CU (B) and B-B (C), and HPLC yields of macrocycles (D, E) during milling and after aging. The content of the dimers is reported as the MS abundance for triplicate measurements ($n = 3$) ± standard deviation, linear fit is expressed as dashed lines. The yields of macrocycles are presented as mean values obtained in a series of replicated experiments ($2 \leq n \leq 4$) with confidence intervals. More details are provided in the Supplementary Information, Table S18 and pages S30-S34.

Further understanding of the dynamic processes and interconversion of intermediates occurring at the milling stage was obtained by tracking the fate of selected short oligomers (Figure 3B-C and Table S18). The changes in content of the characteristic dimers and trimers, and yields of mixHC[8] and cycHC[8] prior to and after the aging stage were determined by HPLC-MS and HPLC-UV analyses. The collected data confirmed that coupling between the CU monomers is kinetically preferred and occurs at the initial phase of the polycondensation reaction. Thus, the quantity of CU-CU dimer drastically increased after 5 min of milling and subsequently underwent rapid decay (Figure 3B). Such fast dynamics and decay was absent for the biotin units reflecting a major difference in condensation between biotin and CU. In contrast to CU, the condensation of the biotin units to respective dimer B-B reached in the beginning of reaction its maximum and probably acts as a transient intermediate (Figure 3B-C). Similar behaviour was observed with the respective trimers (Table S18).The yields of the macrocycles generated at the milling stage did not exceed 20%, but greatly increased during aging (Figure 3D-E). Notably, the macrocyclic content in the aged mixtures is significantly affected by milling duration, when monomer shuffling occurs. Thus, aging of the short-milled (5 minutes) reaction mixture, which contained mainly homomeric CU oligomers, resulted in the ripening of cycHC[8] as the dominant product (55% yield), along with a minor quantity of mixHC[8] (16% yield). However, fast reversible C–N bond formation and cleavage during milling caused rapid dynamic changes in the oligomeric profile with a random distribution of the biotin units. Upon prolonged milling (60 min, see Tables S14-S15), the yield of mixHC[8] notably increased from 16% to 37%, with a concurrent decrease in the yield of cycHC[8] to 38%, resulting in a 1:1 product ratio. Finally, close examination of the aging duration (Table S15) revealed that the maximum content of mixHC[8] was achieved in 3 hours, when the self-assembly process was essentially complete.

The developed mechanochemical procedure significantly surpassed mixHC[8] synthesis in solution, yielding superior selectivity and conversion rates (see S35–S38). Solution-state processes are affected by diffusion with diffusion constants varying for monomers,

aggregates, and oligomeric intermediates due to size difference. In mechanochemistry, reaction rates do not directly depend on the molecular size of the intermediates, but rather on the number of molecular collisions.[47] In addition to the chemical advantages, solvent-free synthesis produces less waste (PMI = 4) compared to reaction in solution (PMI = 306), and is more sustainable based on the respective green metrics (see S35-S38).[32]

Diastereoisomeric (–)- and (+)-mixHC[8]s were synthesized via condensation of either (*R*,*R*)-CU or (*S*,*S*)-CU with (*S*,*S*,*R*)-B, and isolated in 16% and 11% yields, with the purity reaching 88% and 90%, respectively, determined by quantitative NMR (S39–S58).

Anion binding properties

The electron-deficient cavity of HCs enables encapsulation of suitably sized anionic guests.[12] Efficient anion recognition has been reported for bambusurils,[22,48–51] heterobambusurils,[52] biotinurils,[53,54] and cycHCs.[11] We were fortunate to obtain single crystals of the PF_6^- inclusion complex with (−)-mixHC[8] (Figure 4A, S59–S65). DFT modelling study of mixHC[8] diastereomers (S66–S78) revealed clear differences in their conformations (Figure 4B). The cavity, which is mainly surrounded by CU units, is mostly distorted by biotin position. Therefore, its influence on the anion binding properties was evaluated via comparison of the three HC[8] hosts.

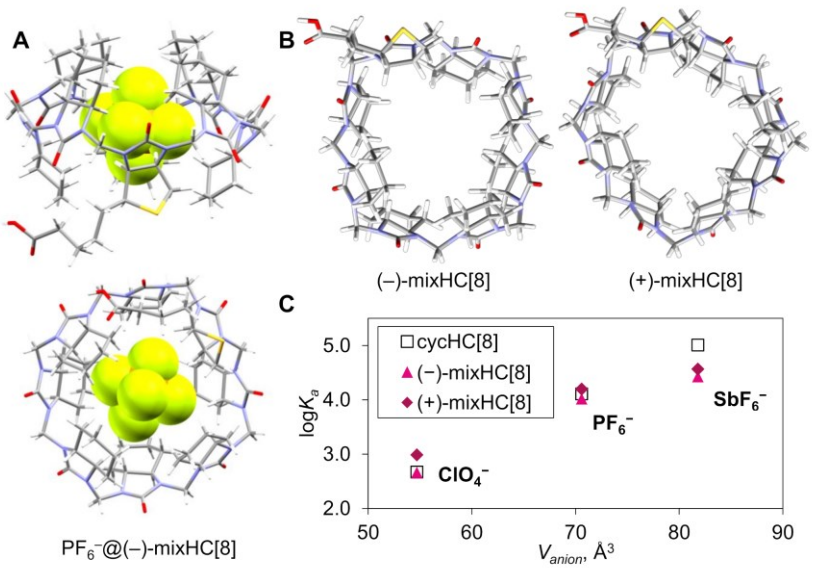

Figure 4. PF_6^-@(–)-mixHC[8] inclusion complex from SC-XRD (A). DFT low-energy structures of (-) and (+)-mixHC[8] diastereomers (B). Correlation between anion volumes (V_{anion}) and association

constants (logK_a), determined by ITC for complexes with (TBA)ClO_4, (TBA)PF_6 (TBA = tetrabutylammonium) and $NaSbF_6$ salts in methanol using a one set of sites model (C).

Encapsulation of the selected anions by the new mixHC[8]s was studied by ITC (Figure 4C, Table S25, Figures S44-S57); the data for cycHC[8] was available from previous work.[11] Complexation between the mono-biotinylated macrocycles and selected chaotropic anions (ClO_4^-, PF_6^- and SbF_6^-) in methanol and a methanol-water mixture (1:1) occurred as an exothermic enthalpy-driven process. The association constants for PF_6^- were greater than that of ClO_4^- in both media, which explains the better templating properties of PF_6^-. Noticeably, the differences between the affinities of the three HC[8] derivatives are the smallest for templating PF_6^- anion, while for ClO_4^- and SbF_6^- either (+)-mixHC[8] or cycHC[8], respectively, exhibit stronger binding. The noted dissimilarities highlight distinctions in the cavities and steric accessibility of these host compounds with potential in a diverse array of applications with unique guest-binding properties.

Selective capture of perchlorate by immobilized mixHC[8]

The new mixHC[8] can be utilized to afford functional materials, which was showcased by the selective removal of perchlorates from contaminated soil samples. Perchlorate is a persistent pollutant that adversely affects human health by interfering with thyroid hormone production, and occurs in soil, ground water, and food.[40,41] The accumulation of perchlorate in fertilizers, soil and irrigation water leads to increased plant uptake and subsequent food-chain transfer.[55,56] This pollutant has been found in various environmental matrices and typically originates from human activities.

The carboxylate side-chain of mixHC[8] enabled its facile covalent immobilization on the surface of 3-aminopropyl silica gel (APS, Figure 5A).[57] The resulting solid perchlorate-extracting material (mixHC[8]-APS) contained ca. 12% (w/w) of mixHC[8], based on infrared spectroscopic analysis (Figure 5B, Figure S58). To prove the removal of perchlorate in the presence of other minerals, a regolith simulant[58] was employed as the matrix of the known composition, and spiked with (TBA)ClO_4, imitating contamination with perchlorate (1% w/w). The obtained model mixture contained cations (Ca^{2+}, Mg^{2+},

Fe^{2+}, Fe^{3+}), oxides and kosmotropic anions (SO_4^{2-}, CO_3^{2-}), but was essentially free of the organic matter (Table S27). According to ion chromatography analysis (Tables S26, S28, Figures S59-S62), the methanolic extract of the contaminated matrix contained primarily perchlorate and sulfate, the latter arising from the $MgSO_4$ component (Table S27). Treatment of the methanolic extract with solid mixHC[8]-APS resulted in complete removal of ClO_4^- in contrast to non-modified APS, which removed ca. 15% ClO_4^- (Figure 5C, Table S28, Figure S62).

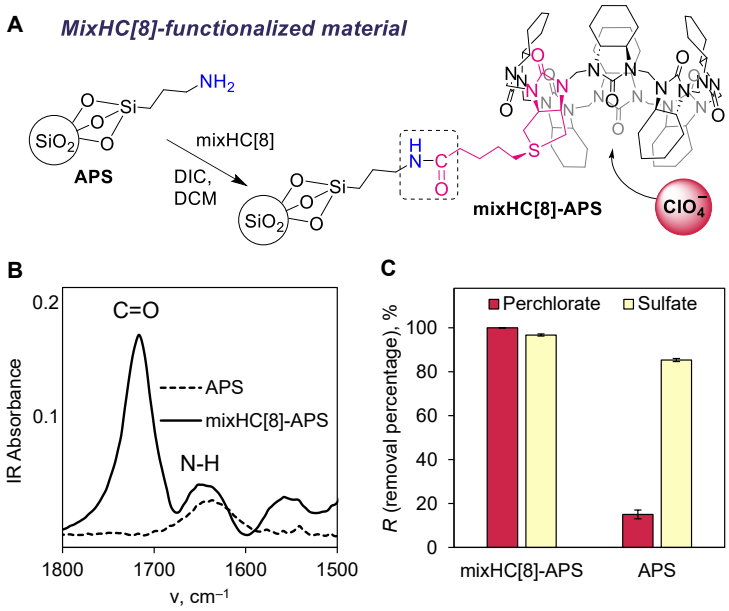

Figure 5. Immobilization of mixHC[8] on APS (A), DIC – *N,N'*-diisopropylcarbodiimide, DCM (dichloromethane); characterization of material by IR (b) and perchlorate removal from spiked mineral matrix using mixHC[8]-APS and non-modified APS, determined by ion chromatography (c). The error bars represent the standard deviation between the parallel experiments ($n \geq 2$).

Extraction of sulfate occurred with similar efficiency (ca. 85–97%) using both APS and mixHC[8]-APS materials, demonstrating that mixHC[8] is not the main contributor responsible for the capture of SO_4^{2-}. The absence of mixHC[8] affinity toward sulfate was additionally confirmed by an ITC experiment (Table S25, Figures S50 and S57).

The captured perchlorate was easily removed by washing mixHC[8]-APS material with water, taking advantage of the weaker binding in the aqueous medium, which demonstrates the potential for the material's reusability[59].

Conclusions

An efficient mechanochemical protocol for the synthesis of the enantiopure mono-biotinylated hemicucurbit[8]urils was developed. The process involves two stages: (i) the mechanochemically-assisted and acid-catalyzed polycondensation of D-biotin, (*R,R*)- or (*S,S*)-cyclohexa-1,2-diylurea and formaldehyde; and (ii) the aging step, in which a template-driven self-assembly of linear-chain oligomers into macrocycles takes place. Screening experiments uncovered the key process and chemical parameters affecting the self-assembly: the ratio of the monomers, loading of acid catalyst, and the nature of the templating anion. The present study offers insight into the complex mixture of oligomeric intermediates, including their interconversion and self-organization processes en route to the macrocyclic products. HPLC-MS analysis of short oligomers revealed differences in condensation kinetics of paraformaldehyde with biotin and cyclohexyl-1,2-urea to homomeric dimers under mechanochemical agitation. The faster condensation of cyclohexyl-1,2-urea led to amplification of the homomeric cycHC[8] during aging for shortly agitated reaction mixtures. On the contrary, upon prolonged mechanochemical agitation, that ensures sufficient shuffling of monomers, higher efficiency in formation of the chimeric mixHC[8] in 37% yield was achieved. The solid-state, self-assembling approach allowed fine-tuning of the composition of the rich dynamic covalent library and directing self-assembly processes beyond statistical distribution. Diastereomeric (−)- and (+)-mixHC[8]s were isolated and their structures were characterized by DFT, NMR and SC-XRD methods. Furthermore, comparison of their affinities to chaotropic anions pointed at specific binding differences, which makes the chimeric family of HC[8] appealing for host-guest chemistry. The biotin carboxylate group of the new mixHC[8] enabled its facile covalent immobilization on aminated silica. The functional material obtained was employed in the selective capture of anions, as demonstrated by the complete removal of perchlorate from an extract of a mineral model mixture. Further applications of these chiral chimeric hemicucurbiturils are currently studied.

Author information

Corresponding Author

Riina Aav, Tallinn University of Technology, Department of Chemistry and Biotechnology, Akadeemia tee 15, Tallinn 12618, Estonia; e-mail: riina.aav@taltech.ee.

Author Contributions

‡These authors contributed equally. All authors contributed to the manuscript's preparation and have provided their approval for the final version of the manuscript. The authors' specific contributions are as follows: E. S.-T. was the main contributor for the development of the synthesis and mixHCs characterization, and participated in binding studies; T.J. was the main contributor of the chemical analysis, binding, immobilization, and perchlorate removal studies; P.T. and S.P. contributed to perchlorate removal; K.-M.L, K.S. and J.V.N. to the synthesis; J.M., J.S.W. and K.R. to SC-XRD analysis; R.R and M.Ö. to computational studies; L.U. to script for MS data analysis and binding studies; M.V to assessment of combinatorics; K.S and J.V.N. to synthesis; V.R. to NMR analysis; D.K. to conceptualization of the synthesis, perchlorate removal, and assessment of green metrics; R.A. to conceptualization of the overall research, data analysis, writing and supervision.

Funding Sources

The research by R.A., L.U., D.K., J.S.W. and K.R. was funded by the European Union's H2020- FETOPEN grant 828779 (INITIO). E.S.-T., T.J., K.-M.L., J.V.N, J.M., R.R. and M.Ö. were financed by the Estonian Research Council grants PRG399 and PRG2169. R.A. was funded by the Ministry of Education and Research through Centre of Excellence in Circular Economy for Strategic Mineral and Carbon Resources (01.01.2024–31.12.2030, TK228). The authors also acknowledge COST Action CA18112 "Mechanochemistry for Sustainable Industry" for supporting research in mechanochemistry.

Acknowledgements

Authors would like to thank Jasper Adamson and Indrek Reile for input to NMR analysis.

Note

This research has been filed for patent application EP23181344.5 “Method of preparation of chimeric hemicucurbit[n]urils, derivatives, and uses thereof”, Priority date: 26.06.2023

Abbreviations

APS, 3-aminopropyl silica gel; CU, (*R*,*R*)- or (*S*,*S*)-*N*,*N*’-cyclohexa-1,2-diylurea; cycHC[8], cyclohexanohemicucurbit[8]uril; DCC, dynamic covalent chemistry; DCL, dynamic covalent library; DCM, dichloromethane; DFT, density functional theory; DIC, *N*,*N*’-diisopropylcarbodiimide; HC, hemicucurbituril; HPLC, high-performance liquid chromatography; HRMS, high-resolution mass spectrometry; ITC, isothermal titration calorimetry; mixHC[8], mono-biotinylated cyclohexanohemicucurbit[8]uril; MS, mass spectrometry; NMR, nuclear magnetic resonance; PMI, process mass intensity; RSM, response surface methodology; SC-XRD, single crystal X-ray diffraction; TBA, tetrabutylammonium.

References

(1) Schnitzer, T.; Preuss, M. D.; van Basten, J.; Schoenmakers, S. M. C.; Spiering, A. J. H.; Vantomme, G.; Meijer, E. W. How Subtle Changes Can Make a Difference: Reproducibility in Complex Supramolecular Systems. Angewandte Chemie 2022, 134 (41), e202206738. https://doi.org/10.1002/ange.202206738.

(2) Yamaoki, Y.; Nagata, T.; Kondo, K.; Sakamoto, T.; Takami, S.; Katahira, M. Shedding Light on the Base-Pair Opening Dynamics of Nucleic Acids in Living Human Cells. Nat Commun 2022, 13 (1), 7143. https://doi.org/10.1038/s41467-022-34822-4.

(3) Kwon, T.; Song, B.; Nam, K. W.; Stoddart, J. F. Mechanochemical Enhancement of the Structural Stability of Pseudorotaxane Intermediates in the Synthesis of Rotaxanes. J. Am. Chem. Soc. 2022, 144 (28), 12595–12601. https://doi.org/10.1021/jacs.2c00515.

(4) Dračínský, M.; Hurtado, C. S.; Masson, E.; Kaleta, J. Stuffed Pumpkins: Mechanochemical Synthesis of Host–Guest Complexes with Cucurbit[7]Uril. Chemical Communications 2021, 57 (17), 2132–2135. https://doi.org/10.1039/D1CC00240F.

(5) Friščić, T.; Mottillo, C.; Titi, H. M. Mechanochemistry for Synthesis. Angewandte Chemie 2020, 132 (3), 1030–1041. https://doi.org/10.1002/ange.201906755.

(6) Cuccu, F.; De Luca, L.; Delogu, F.; Colacino, E.; Solin, N.; Mocci, R.; Porcheddu, A. Mechanochemistry: New Tools to Navigate the Uncharted Territory of "Impossible" Reactions. ChemSusChem 2022, 15 (17), e202200362. https://doi.org/10.1002/cssc.202200362.

(7) Reynes, J. F.; Isoni, V.; García, F. Tinkering with Mechanochemical Tools for Scale Up. Angewandte Chemie International Edition 2023, 62 (44), e202300819. https://doi.org/10.1002/anie.202300819.

(8) Kaabel, S.; Aav, R. Templating Effects in the Dynamic Chemistry of Cucurbiturils and Hemicucurbiturils. Israel Journal of Chemistry 2018, 58 (3–4), 296–313. https://doi.org/10.1002/ijch.201700106.

(9) Lehn, J.-M. Dynamic Combinatorial Chemistry and Virtual Combinatorial Libraries. Chemistry – A European Journal 1999, 5 (9), 2455–2463. https://doi.org/10.1002/(SICI)1521-3765(19990903)5:9<2455::AID-CHEM2455>3.0.CO;2-H.

(10) Corbett, P. T.; Leclaire, J.; Vial, L.; West, K. R.; Wietor, J.-L.; Sanders, J. K. M.; Otto, S. Dynamic Combinatorial Chemistry. Chem. Rev. 2006, 106 (9), 3652–3711. https://doi.org/10.1021/cr020452p.

(11) Kaabel, S.; Adamson, J.; Topić, F.; Kiesilä, A.; Kalenius, E.; Öeren, M.; Reimund, M.; Prigorchenko, E.; Lõokene, A.; Reich, H. J.; Rissanen, K.; Aav, R. Chiral Hemicucurbit[8]Uril as an Anion Receptor: Selectivity to Size, Shape and Charge Distribution. Chem. Sci. 2017, 8 (3), 2184–2190. https://doi.org/10.1039/C6SC05058A.

(12) Andersen, N. N.; Lisbjerg, M.; Eriksen, K.; Pittelkow, M. Hemicucurbit[n]Urils and Their Derivatives – Synthesis and Applications. Israel Journal of Chemistry 2018, 58 (3–4), 435–448. https://doi.org/10.1002/ijch.201700129.
(13) Lisbjerg, M.; Jessen, B. M.; Rasmussen, B.; Nielsen, B. E.; Madsen, A. Ø.; Pittelkow, M. Discovery of a Cyclic 6 + 6 Hexamer of D-Biotin and Formaldehyde. Chem. Sci. 2014, 5 (7), 2647–2650. https://doi.org/10.1039/C4SC00990H.
(14) Havel, V.; Yawer, M. A.; Sindelar, V. Real-Time Analysis of Multiple Anion Mixtures in Aqueous Media Using a Single Receptor. Chem. Commun. 2015, 51 (22), 4666–4669. https://doi.org/10.1039/C4CC10108A.
(15) Yawer, M. A.; Havel, V.; Sindelar, V. A Bambusuril Macrocycle That Binds Anions in Water with High Affinity and Selectivity. Angewandte Chemie International Edition 2015, 54 (1), 276–279. https://doi.org/10.1002/anie.201409895.
(16) Lizal, T.; Sindelar, V. Bambusuril Anion Receptors. Isr. J. Chem. 2018, 58 (3–4), 326–333. https://doi.org/10.1002/ijch.201700111.
(17) Kaabel, S.; Stein, R. S.; Fomitšenko, M.; Järving, I.; Friščić, T.; Aav, R. Size-Control by Anion Templating in Mechanochemical Synthesis of Hemicucurbiturils in the Solid State. Angewandte Chemie International Edition 2019, 58 (19), 6230–6234. https://doi.org/10.1002/anie.201813431.
(18) Prigorchenko, E.; Öeren, M.; Kaabel, S.; Fomitšenko, M.; Reile, I.; Järving, I.; Tamm, T.; Topić, F.; Rissanen, K.; Aav, R. Template-Controlled Synthesis of Chiral Cyclohexylhemicucurbit[8]Uril. Chem. Commun. 2015, 51 (54), 10921–10924. https://doi.org/10.1039/C5CC04101E.
(19) Zeng, Q.; Long, Q.; Lu, J.; Wang, L.; You, Y.; Yuan, X.; Zhang, Q.; Ge, Q.; Cong, H.; Liu, M. Synthesis of a Novel Aminobenzene-Containing Hemicucurbituril and Its Fluorescence Spectral Properties with Ions. Beilstein J. Org. Chem. 2021, 17 (1), 2840–2847. https://doi.org/10.3762/bjoc.17.195.
(20) Wang, L.; Han, J.; Pan, R.; Yuan, X.; You, Y.; Cen, X.; Zhang, Q.; Ge, Q.; Cong, H.; Liu, M. Synthesis of Hybrid Thiohemicucurbiturils. Tetrahedron Letters 2022, 101, 153918. https://doi.org/10.1016/j.tetlet.2022.153918.
(21) Maršálek, K.; Šindelář, V. Monofunctionalized Bambus[6]Urils and Their Conjugates with Crown Ethers for Liquid–Liquid Extraction of Inorganic Salts. Org. Lett. 2020, 22 (4), 1633–1637. https://doi.org/10.1021/acs.orglett.0c00216.
(22) De Simone, N. A.; Chvojka, M.; Lapešová, J.; Martínez-Crespo, L.; Slávik, P.; Sokolov, J.; Butler, S. J.; Valkenier, H.; Šindelář, V. Monofunctionalized Fluorinated Bambusurils and Their Conjugates for Anion Transport and Extraction. J. Org. Chem. 2022, 87 (15), 9829–9838. https://doi.org/10.1021/acs.joc.2c00870.
(23) Del Mauro, A.; Lapešová, J.; Rando, C.; Šindelář, V. Merging Bambus[6]Uril and Biotin[6]Uril into an Enantiomerically Pure Monofunctionalized Hybrid Macrocycle. Org. Lett. 2024, 26 (1), 106–109. https://doi.org/10.1021/acs.orglett.3c03715.
(24) Langerreiter, D.; Kostiainen, M. A.; Kaabel, S.; Anaya-Plaza, E. A Greener Route to Blue: Solid-State Synthesis of Phthalocyanines. Angewandte Chemie International Edition 2022, 61 (42), e202209033. https://doi.org/10.1002/anie.202209033.

(25) Pascu, M.; Ruggi, A.; Scopelliti, R.; Severin, K. Synthesis of Borasiloxane-Based Macrocycles by Multicomponent Condensation Reactions in Solution or in a Ball Mill. Chem. Commun. 2012, 49 (1), 45–47. https://doi.org/10.1039/C2CC37538A.
(26) Sim, Y.; Shi, Y. X.; Ganguly, R.; Li, Y.; García, F. Mechanochemical Synthesis of Phosphazane-Based Frameworks. Chemistry – A European Journal 2017, 23 (47), 11279–11285. https://doi.org/10.1002/chem.201701619.
(27) Xi, H.-T.; Zhao, T.; Sun, X.-Q.; Miao, C.-B.; Zong, T.; Meng, Q. Rapid and Efficient Solvent-Free Synthesis of Cyclophanes Based on Bipyridinium under Mechanical Ball Milling. RSC Adv. 2012, 3 (3), 691–694. https://doi.org/10.1039/C2RA22802E.
(28) Kunde, T.; Pausch, T.; Guńka, P. A.; Krzyżanowski, M.; Kasprzak, A.; Schmidt, B. M. Fast, Solvent-Free Synthesis of Ferrocene-Containing Organic Cages via Dynamic Covalent Chemistry in the Solid State. Chem. Sci. 2022, 13 (10), 2877–2883. https://doi.org/10.1039/D1SC06372C.
(29) Shy, H.; Mackin, P.; Orvieto, A. S.; Gharbharan, D.; Peterson, G. R.; Bampos, N.; Hamilton, T. D. The Two-Step Mechanochemical Synthesis of Porphyrins. Faraday Discuss. 2014, 170 (0), 59–69. https://doi.org/10.1039/C3FD00140G.
(30) Su, Q.; Hamilton, T. D. Extending Mechanochemical Porphyrin Synthesis to Bulkier Aromatics: Tetramesitylporphyrin. Beilstein J. Org. Chem. 2019, 15 (1), 1149–1153. https://doi.org/10.3762/bjoc.15.111.
(31) Weisstein, E. W. Necklace. https://mathworld.wolfram.com/ (accessed 2024-04-16).
(32) McElroy, C. R.; Constantinou, A.; Jones, L. C.; Summerton, L.; Clark, J. H. Towards a Holistic Approach to Metrics for the 21st Century Pharmaceutical Industry. Green Chem. 2015, 17 (5), 3111–3121. https://doi.org/10.1039/C5GC00340G.
(33) Friščić, T.; Childs, S. L.; Rizvi, S. A. A.; Jones, W. The Role of Solvent in Mechanochemical and Sonochemical Cocrystal Formation: A Solubility-Based Approach for Predicting Cocrystallisation Outcome. CrystEngComm 2009, 11 (3), 418–426. https://doi.org/10.1039/B815174A.
(34) Do, J.-L.; Friščić, T. Chemistry 2.0: Developing a New, Solvent-Free System of Chemical Synthesis Based on Mechanochemistry. Synlett 2017, 28 (16), 2066–2092. https://doi.org/10.1055/s-0036-1590854.
(35) Belenguer, A. M.; Lampronti, G. I.; De Mitri, N.; Driver, M.; Hunter, C. A.; Sanders, J. K. M. Understanding the Influence of Surface Solvation and Structure on Polymorph Stability: A Combined Mechanochemical and Theoretical Approach. J. Am. Chem. Soc. 2018, 140 (49), 17051–17059. https://doi.org/10.1021/jacs.8b08549.
(36) Prigorchenko, E.; Kaabel, S.; Narva, T.; Baškir, A.; Fomitšenko, M.; Adamson, J.; Järving, I.; Rissanen, K.; Tamm, T.; Aav, R. Formation and Trapping of the Thermodynamically Unfavoured Inverted-Hemicucurbit[6]Uril. Chem. Commun. 2019, 55 (63), 9307–9310. https://doi.org/10.1039/C9CC04990H.
(37) Myers, R. H.; Montgomery, D. C.; Anderson-Cook, C. M. Response Surface Methodology: Process and Product Optimization Using Designed Experiments; John Wiley & Sons, 2016.
(38) Czapla, M.; Skurski, P. Strength of the Lewis–Brønsted Superacids Containing In, Sn, and Sb and the Electron Binding Energies of Their Corresponding Superhalogen

Anions. J. Phys. Chem. A 2015, 119 (51), 12868–12875. https://doi.org/10.1021/acs.jpca.5b10205.
(39) Bour, C.; Guillot, R.; Gandon, V. First Evidence for the Existence of Hexafluoroantimonic(V) Acid. Chemistry – A European Journal 2015, 21 (16), 6066–6069. https://doi.org/10.1002/chem.201500334.
(40) Urbansky, E. T. Perchlorate as an Environmental Contaminant. Environ Sci & Potlut Res 2002, 9 (3), 187–192. https://doi.org/10.1007/BF02987487.
(41) Kumarathilaka, P.; Oze, C.; Indraratne, S. P.; Vithanage, M. Perchlorate as an Emerging Contaminant in Soil, Water and Food. Chemosphere 2016, 150, 667–677. https://doi.org/10.1016/j.chemosphere.2016.01.109.
(42) Sigel, H.; Scheller, K. H. Metal Ion Complexes of D-Biotin in Solution. Stability of the Stereoselective Thioether Coordination. Journal of Inorganic Biochemistry 1982, 16 (4), 297–310. https://doi.org/10.1016/S0162-0134(00)80266-4.
(43) Aoki, K.; Saenger, W. Interactions of Biotin with Metal Ions. X-Ray Crystal Structure of the Polymeric Biotin-Silver(i) Nitrate Complex: Metal Bonding to Thioether and Ureido Carbonyl Groups. Journal of Inorganic Biochemistry 1983, 19 (3), 269–273. https://doi.org/10.1016/0162-0134(83)85031-4.
(44) Altaf, M.; Stoeckli-Evans, H. Chiral One- and Two-Dimensional Silver(I)–Biotin Coordination Polymers. Acta Cryst C 2013, 69 (2), 127–137. https://doi.org/10.1107/S0108270113000322.
(45) Lehn, J.-M. Perspectives in Chemistry—Steps towards Complex Matter. Angewandte Chemie International Edition 2013, 52 (10), 2836–2850. https://doi.org/10.1002/anie.201208397.
(46) Ustrnul, L.; Jarg, T.; Jantson, M.; Osadchuk, I.; Anton, L.; Aav, R. MatchMass: A Web-Based Tool for Efficient Mass Spectrometry Data Analysis. ChemRxiv April 26, 2024. https://doi.org/10.26434/chemrxiv-2024-9j8n7.
(47) Ma, X.; Yuan, W.; Bell, S. E. J.; James, S. L. Better Understanding of Mechanochemical Reactions: Raman Monitoring Reveals Surprisingly Simple 'Pseudo-Fluid' Model for a Ball Milling Reaction. Chem. Commun. 2014, 50 (13), 1585–1587. https://doi.org/10.1039/C3CC47898J.
(48) Jašíková, L.; Rodrigues, M.; Lapešová, J.; Lízal, T.; Šindelář, V.; Roithová, J. Bambusurils as a Mechanistic Tool for Probing Anion Effects. Faraday Discuss. 2019, 220 (0), 58–70. https://doi.org/10.1039/C9FD00038K.
(49) Sokolov, J.; Štefek, A.; Šindelář, V. Functionalized Chiral Bambusurils: Synthesis and Host-Guest Interactions with Chiral Carboxylates. ChemPlusChem 2020, 85 (6), 1307–1314. https://doi.org/10.1002/cplu.202000261.
(50) Itterheimová, P.; Bobacka, J.; Šindelář, V.; Lubal, P. Perchlorate Solid-Contact Ion-Selective Electrode Based on Dodecabenzylbambus[6]Uril. Chemosensors 2022, 10 (3), 115. https://doi.org/10.3390/chemosensors10030115.
(51) Rando, C.; Vázquez, J.; Sokolov, J.; Kokan, Z.; Nečas, M.; Šindelář, V. Highly Efficient and Selective Recognition of Dicyanoaurate(I) by a Bambusuril Macrocycle in Water. Angewandte Chemie International Edition 2022, 61 (43), e202210184. https://doi.org/10.1002/anie.202210184.

(52) Reany, O.; Mohite, A.; Keinan, E. Hetero-Bambusurils. Israel Journal of Chemistry 2018, 58 (3–4), 449–460. https://doi.org/10.1002/ijch.201700138.
(53) Lisbjerg, M.; Nielsen, B. E.; Milhøj, B. O.; Sauer, S. P. A.; Pittelkow, M. Anion Binding by Biotin[6]Uril in Water. Org. Biomol. Chem. 2015, 13 (2), 369–373. https://doi.org/10.1039/C4OB02211D.
(54) Andersen, N. N.; Eriksen, K.; Lisbjerg, M.; Ottesen, M. E.; Milhøj, B. O.; Sauer, S. P. A.; Pittelkow, M. Entropy/Enthalpy Compensation in Anion Binding: Biotin[6]Uril and Biotin-l-Sulfoxide[6]Uril Reveal Strong Solvent Dependency. J. Org. Chem. 2019, 84 (5), 2577–2584. https://doi.org/10.1021/acs.joc.8b02797.
(55) Calderón, R.; Palma, P.; Arancibia-Miranda, N.; Kim, U.-J.; Silva-Moreno, E.; Kannan, K. Occurrence, Distribution and Dynamics of Perchlorate in Soil, Water, Fertilizers, Vegetables and Fruits and Associated Human Exposure in Chile. Environ Geochem Health 2022, 44 (2), 527–535. https://doi.org/10.1007/s10653-020-00680-6.
(56) Chen, Y.; Zhu, Z.; Wu, X.; Zhang, D.; Tong, J.; Lin, Y.; Yin, L.; Li, X.; Zheng, Q.; Lu, S. A Nationwide Investigation of Perchlorate Levels in Staple Foods from China: Implications for Human Exposure and Risk Assessment. Journal of Hazardous Materials 2022, 439, 129629. https://doi.org/10.1016/j.jhazmat.2022.129629.
(57) Tabakci, M. Immobilization of Calix[6]Arene Bearing Carboxylic Acid and Amide Groups on Aminopropyl Silica Gel and Its Sorption Properties for Cr(VI). J Incl Phenom Macrocycl Chem 2008, 61 (1), 53–60. https://doi.org/10.1007/s10847-007-9392-2.
(58) Cannon, K. M.; Britt, D. T.; Smith, T. M.; Fritsche, R. F.; Batcheldor, D. Mars Global Simulant MGS-1: A Rocknest-Based Open Standard for Basaltic Martian Regolith Simulants. Icarus 2019, 317, 470–478. https://doi.org/10.1016/j.icarus.2018.08.019.
(59) Shalima, T.; Mishra, K. A.; Kaabel, S.; Ustrnul, L.; Bartkova, S.; Tõnsuaadu, K.; Heinmaa, I.; Aav, R. Cyclohexanohemicucurbit[8]Uril Inclusion Complexes With Heterocycles and Selective Extraction of Sulfur Compounds From Water. Frontiers in Chemistry 2021, 9.